Photocatalytic Approach for CO_2 Fixation

Kazuhiko Maeda

Abstract In order to address the depletion of fossil fuels and the serious environmental problems accompanying their combustion and the concomitant CO_2 emission, large-scale chemical conversion of CO_2 into energy-rich materials would be an ultimate solution, and several reactions have been proposed. There have been a lot of challenges that have to be addressed in this field of research, but several breakthroughs have been achieved in recent 10 years. In this chapter, photocatalytic CO_2 reduction systems, which are of particular importance, are reviewed, with a focus on both homogeneous and heterogeneous aspects.

Keywords Fossil fuels · CO_2 reduction · Carbon monoxide · Formic acid · Metal complex · Photocatalysis · Photocatalyst · Sunlight · Isotope · Rhenium · Dimethylformamide (DMF) · Triethanolamine (TEOA) · Quantum yield · One electron reduced (OER) species · Turnover number · Electron donor · Supramolecular metal complex · Intramolecular electron transfer · One electron reduced (OER) species · Intramolecular electron transfer · Ruthenium · Manganese · Chlorophylls · Resonance energy transfer · Conjugation · Mesoporous silica · Light-harvesting · Semiconductor · Water oxidation · Langmuir-Hinshelwood type mechanism · Perovskite · Cocatalyst · Silver · Overpotential · Water splitting · Layered double hydroxide (LDH) · Heterogeneous photocatalysis · Acetonitrile · Polymer · Carbon nitride · Visible light · Carbon nitride · Visible light · Action spectrum · Z-scheme · Natural photosynthesis · Sensitizer · Hydrogen evolution · Electron-hole recombination

---

K. Maeda (✉)
Department of Chemistry, Tokyo Institute of Technology, 2-12-1-NE-2 Ookayama,
Meguro-ku, Tokyo 152-8550, Japan
e-mail: maedak@chem.titech.ac.jp

M. Sugiyama et al. (eds.), *Solar to Chemical Energy Conversion*,
Lecture Notes in Energy 32, DOI 10.1007/978-3-319-25400-5_10

1 Introduction

1.1 Research Background

Photocatalytic CO_2 fixation into energy-rich chemicals such as carbon monoxide and formic acid has attracted attention in order to address the depletion of carbon resources and the suppression of global warming as well as to accomplish the CO_2-reduction half cycle in artificial photosynthesis [1, 2]. Because CO_2 is a very stable molecule, the reduction of CO_2 remains a big challenge; it requires a high potential to electrochemically reduce CO_2 by one electron (–1.9 V vs. NHE at pH 7). On the other hand, the required potential for CO_2 reduction can be reduced if one utilizes multi-electron process. For example, the potentials of two-electron reduction of CO_2 into formic acid and CO are –0.61 and –0.53 V (vs. NHE at pH 7), respectively, approximately 1.3 V more positive than the potential required to drive one-electron reduction of CO_2.

$$\begin{aligned}
&CO_2 + 2H^+ + 2e^- \rightarrow HCOOH \quad E^\circ = -0.61V\\
&CO_2 + 2H^+ + 2e^- \rightarrow CO + H_2O \quad E^\circ = -0.53V\\
&CO_2 + 4H^+ + 4e^- \rightarrow HCHO + H_2O \quad E^\circ = -0.48V\\
&CO_2 + 6H^+ + 6e^- \rightarrow CH_3OH + H_2O \quad E^\circ = -0.38V\\
&CO_2 + 8H^+ + 8e^- \rightarrow CH_4 + 2H_2O \quad E^\circ = -0.24V
\end{aligned}$$

Thus, a catalyst that allows one to promote multi-electron transfer is needed. As described below, certain metal complexes and semiconductors (as well as their composites) work as such (photo)catalysts.

Since the seminal work by Lehn et al. who demonstrated selective CO_2 reduction into CO using Re(I) diimine complexes in 1983 [3], photocatalytic CO_2 reduction has been extensively studied for the purpose of light-to-chemical energy conversion. However, a satisfactory system has yet to be devised to date. As the goal of CO_2 fixation by a photocatalyst is to convert solar energy into chemical energy on a large-scale, a given system has to meet the following requirements.

(1) A given CO_2 fixation system has to be workable under sunlight having low energy density, and to be stable and efficient during long-term operation.
(2) CO_2 reduction has to be promoted while suppressing any side reaction that can occur during the reaction (e.g., H_2 reduction via water reduction).
(3) Water should be used as an electron source.

Unfortunately, no photocatalytic system that satisfies all of the above requirements has been reported to date. Besides, energy conversion scheme via CO_2 reduction where the change in Gibbs energy is positive had not been achieved until very recently. Nevertheless, there were some breakthroughs especially in the last 10 years. This chapter describes recent progress on photocatalytic CO_2 reduction using metal complexes and semiconductors, along with some important early works.

1.2 Some Important Aspects in Photocatalytic CO_2 Fixation Research

One should be careful when reading a literature on photocatalytic CO_2 reduction, as some may be problematic. For example, even though a given CO_2 fixation system is claimed to work in water, quantification of O_2, which is the product of water oxidation, is ambiguously or not described. Besides, it is extremely important in any of photocatalytic CO_2 reduction research to investigate the origin of carbon-containing products by isotope tracer experiments with $^{13}CO_2$, because contaminated carbon species may become such materials upon photo-irradiation especially in a heterogeneous system. For example, using a commercially available titania loaded with nanoparticulate metal promoters as a heterogeneous photocatalyst for CO_2 reduction, it has been revealed that both CO and CH_4 were obtained, but the contribution of surface contaminants to the reaction products cannot be neglected [4]. High turnover number with respect to the amount of catalytically active sites or the photocatalyst itself is also an important indicator to judge whether or not a given reaction photocatalyzes CO_2 reduction. In this section, the author would like to focus on representative, but "reliable" systems in this regard, which are considered important milestones in photocatalytic CO_2 reduction research.

2 Metal Complexes

2.1 Re Diimine Tricarbonyl Type Complexes

In 1983, Lehn et al. reported that *fac*-$[Re(N^\wedge N)(CO)_3X]^+$ (N^N = diimine ligand; X = Cl^-, Br^-) not only works as an efficient CO_2 reduction photocatalyst but also as a catalyst (Scheme 1). These Re(I) complexes selectively produce CO in a dimethylformamide (DMF)/triethanolamine (TEOA) solution. It is noted that even in the presence of water, certain Re(I) complexes are capable of selectively producing CO without noticeable H_2 formation [3].

Follow-up studies have been made to create more active photocatalysts. The chloro ligand on *fac*-$Re(bpy)(CO)_3Cl$ (bpy = 2,2′-bipyridine) undergoes substitution with various phosphorus ligands, PR_3 (R = alkyl, alkoxy, or allyl group),

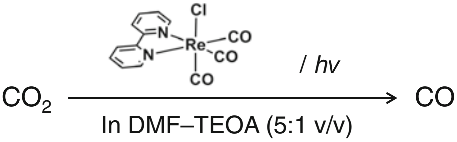

Scheme 1 Photocatalytic CO_2 reduction into CO on *fac*-$[Re(bpy)CO_3Cl]^+$ in a mixed solution of DMF and TEOA

giving *fac*-$[Re(bpy)(CO)_3(PR_3)]^+$ [5]. The photocatalytic activity for CO_2 reduction was found to depend strongly on the phosphorus ligand [6]. For example, *fac*-$[Re(bpy)(CO)_3\{P(OEt)_3\}]^+$ is an efficient photocatalyst for CO formation with a quantum yield (QY) of 38 % at 365 nm [7], which is twice as large compared with that with *fac*-$Re(bpy)(CO)_3Cl$.

The reaction mechanism of photocatalytic CO_2 reduction in a homogeneous system was investigated by Ishitani et al. in detail using three different Re(I) diimine complexes, *fac*-$[Re(bpy)(CO)_3L]$ (L = SCN^- (**1–NCS**), Cl^- (**1–Cl**), and CN^- (**1–CN**)) [8]. The reaction scheme is given in Scheme 2. It has been revealed by means of laser spectroscopy that the initial step of the reaction is the reductive quenching of the triplet metal-to-ligand charge transfer (^{3}MLCT) excited-state of the Re complex by TEOA, generating one-electron reduced (OER) species of the rhenium complex $[Re^I(N^\wedge N^{\bullet-})(CO)_3X]^-$ [9–11]. The corresponding OER species of these complexes play two important roles of capturing CO_2 after loss of the monodentate ligand (L) and of donating the second electron to CO_2 by another OER species without losing L. In the case of **1–NCS,** the corresponding OER species play these two roles in the photocatalytic reaction, resulting in more efficient CO evolution (30 % QY) than that of **1–Cl** (16 % QY), whose OER species are too short-loved to accumulate during the photocatalytic reaction. On the other hand, **1–CN** showed no photocatalytic ability, because the corresponding OER species does not dissociate the CN- ligand. Based on this mechanistic information, the most efficient photocatalytic system was successfully developed using a mixture of *fac*-$[Re(bpy)(CO)_3(CH_3CN)]^+$ and *fac*-$[Re\{4,4'\text{-}(MeO)_2bpy\}(CO)_3\{P(OEt)_3\}]^+$, which respectively work as a catalyst and a redox sensitizer. The QY of this system was 59 % at the optimal condition.

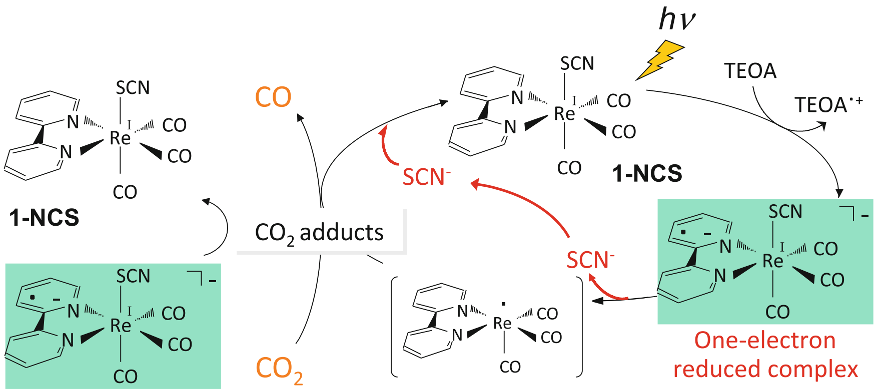

Scheme 2 Photocatalytic reaction mechanism by **1–NCS**. (Reproduced with permission from Ref. [8]. Copyright 2008, American Chemical Society)

Based on the mechanistic study, Ishitani et al. have proposed strategies to develop a highly efficient CO_2 reduction photocatalyst.

(1) Efficient formation of OER species by quenching of ^{3}MLCT excited-state by an electron donor.
(2) Effective production of $[Re(LL^{\bullet -})(CO)_3]$ by dissociation of the ligand from the OER species.
(3) Efficient reduction of CO_2 adduct(s) by another OER species.
(4) Prompt recovery of the starting complex by re-coordination of a ligand after CO formation.

A highly efficient CO_2 reduction has thus been established. However, there still remained unclear point(s) on the reaction mechanism, especially a CO_2 addition step to the Re center. So far, 17-electron species, i.e., $[Re^0(N^\wedge N)(CO)_3]$ and/or $[Re^I(N^\wedge N^{\bullet -})(CO)_3]$ [3, 12–14] and a Re dimer with CO_2 as a bridge ligand [14, 15] have been proposed as possible intermediates derived from reduced Re complexes. However, no clear evidence had been obtained to clarify the mechanism. Another important aspect in photocatalytic CO_2 reduction on Re complexes is that TEOA works as a special electron donor, which enhances catalytic turnover number and selectivity of CO production, compared with other reductants such as triethylamine [16], suggesting a special action of TEOA during the reaction.

Ishitani et al. pointed out that *fac*-$[Re^I(bpy)(CO)_3\{R_2N–CH_2CH_2O–COO\}]$ (R = CH_2CH_2OH) could be a predominant complex in various photocatalytic CO_2 reduction reactions using $[Re^I(N^\wedge N)(CO)_3X]^{n+}$ (X = monodentate ligand; $n = 0, 1$) type complexes in a DMF–TEOA mixed solution (Scheme 3) [17]. A DMF-coordinated complex, *fac*-$[Re^I(bpy)(CO)_3(DMF)]^+$ (**1**), underwent transformation upon addition of TEOA to generate *fac*-$[Re^I(bpy)(CO)_3(OCH_2CH_2NR_2)]$ (**1′**) with an equilibrium constant of 19. Further exposure of **1′** to CO_2 resulted in the generation of **2**, whereas a similar CO_2 treatment of **1** did not. The equilibrium constant between **1′** and **2** ($K = [2]/[1'][CO_2]$) in a CO_2 atmosphere was estimated to be $1.7 \times 10^3\ M^{-1}$, which means the exclusive formation of **2** in the CO_2-saturated mixed solution of DMF and TEOA. This also suggests that even a very low concentration of CO_2 is enough to produce the CO_2–TEOA adduct. Electrochemical analysis indicated the superior CO_2 reduction ability of **2** to **1**. On the basis of these observations,

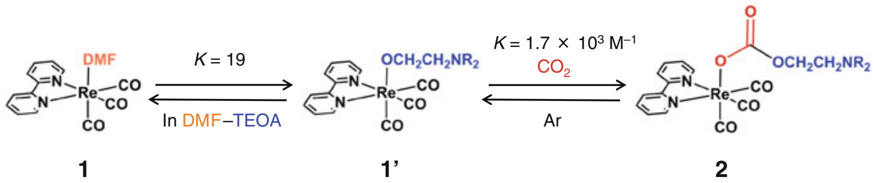

Scheme 3 Structural change of *fac*-$[Re(bpy)CO_3DMF]^+$ in the presence of TEOA and CO_2. (Reproduced with permission from Ref. [17]. Copyright 2013, American Chemical Society)

it was claimed that **2** should be the catalytically active species in many photocatalytic CO_2 reduction systems that have been reported so far, because TEOA was used as an electron donor in these reported systems.

2.2 Supramolecular Metal Complexes

As introduced above, Re(I) diimine complexes work as photocatalysts and electrocatalysts for CO_2 reduction. However, there are several problems in these Re-based complexes including (1) insufficient visible-light-absorption, (2) low stability, and (3) reliance on a strong electron donor. A strategy to address the problems (1) and (2) is to couple a catalytic metal complex with a redox photosensitizer so as to improve the electron transfer process from the excited-state sensitizer to the catalytic unit.

Ishitani et al. prepared a series of Ru(II)−Re(I) binuclear complexes (see Fig. 1), and examined their photocatalytic activities [18]. As shown in Fig. 1, improved photocatalytic activity was obtained with the binuclear complex **[d$_2$Ru-Re]$^{2+}$**, compared to either the corresponding Ru or Re unit alone and a physical mixture of the Ru and Re unit. This is attributed to improved intramolecular electron transfer from the OER species, which were produced following the selective excitation and subsequent reductive quenching of the Ru ^{3}MLCT excited state, to the catalytic Re moiety. It is also noted that photocatalytic responses were extended further into the visible region by applying a Ru moiety as the sensitizing unit.

Another important information obtained from this work is that the photocatalytic abilities of the binuclear complexes with a 4-methyl-4′- [1, 10] phenanthroline-[5,6-d]imidazol-2-yl)bipyridine (abbreviated as BL) bridging ligand, i.e., **[Ru-BL-Re]$^{2+}$** and **[Re-BL-Ru]$^{2+}$**, were much lower than that containing a bpyC$_3$bpy bridging ligand (**[d$_2$Ru-Re]$^{2+}$**). When $(CF_3)_2$bpy or bpy were used as peripheral ligands, the binuclear complexes also had poor photocatalytic ability, giving a turnover numbers (TNs) for CO formation of 3 and 50, respectively, for **[tfbRu-Re]$^{2+}$** and **[b$_2$Ru-Re]$^{2+}$** (data not plotted in Fig. 1). In these metal complexes that showed poorer photocatalytic activity, the intramolecular electron transfer was found to be endothermic, hindering the forward electron transfer and leading to inferior performance. In addition to the endothermic character in the intramolecular electron transfer event, it appears that electron localization on the bridging ligand appears to be another decisive factor. One can assume that, electrons in **[Ru-BL-Re]$^{2+}$** are mainly localized on the Ru end of the bridging ligand, because the energy level of the π* orbital on the phenanthroline-imidazolyl motif of BL is lower than that on the bpy one coordinating to the Re unit. The low electron density on the catalytic Re site in the OER species could account for the low photocatalytic activity of **[Ru-BL-Re]$^{2+}$**.

In the case of **[Re-BL-Ru]$^{2+}$**, in contrast, electron localization must occur on the Re site, which is supposed to contribute to higher photocatalytic activity. It has been reported that photocatalytic CO_2 reduction activities of mononuclear complexes of

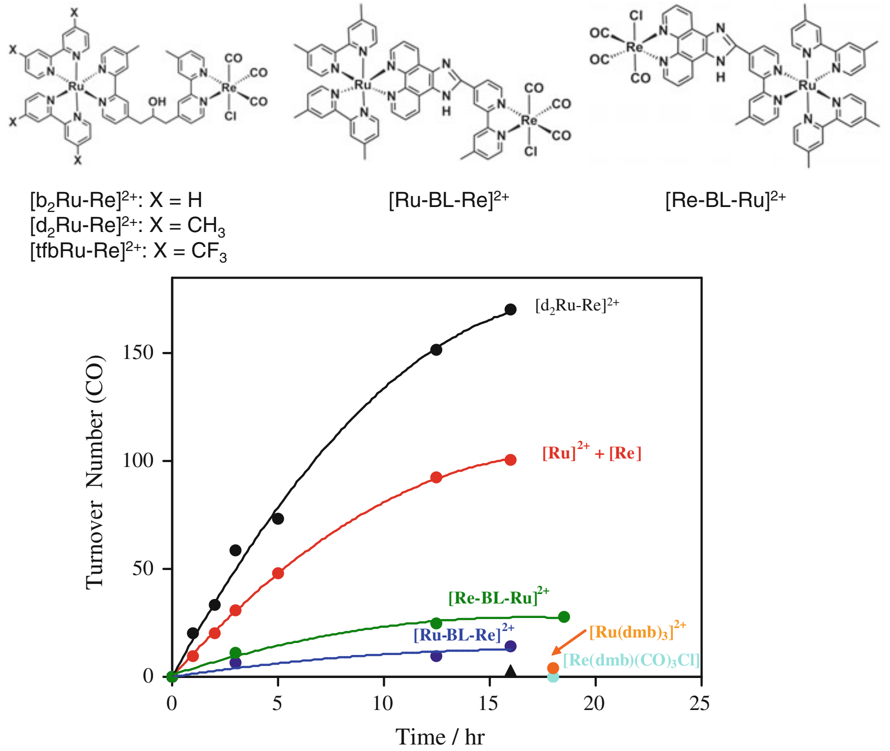

Fig. 1 Photocatalytic activities of supramolecular metal complexes (0.05 mM) for CO formation in a CO_2-saturated DMF–TEOA (5:1 v/v) solution containing 0.1 M 1-Benzyl-1, 4-dihydronicotinamide (BNAH) as a sacrificial electron donor under selective photoexcitation of the Ru moieties (λ > 500 nm). (Reproduced with permission from Ref. [18]. Copyright 2005, American Chemical Society)

fac-[Re(N^N)(CO)$_3$(PR$_3$)]$^+$ (R = an alkyl group) depend strongly on their reduction potentials, $E_{1/2}^{\mathrm{red}}(\mathrm{LL/LL}^{\bullet -})$, and efficient photocatalytic reduction of CO_2 requires $E_{1/2}^{\mathrm{red}}(\mathrm{LL/LL}^{\bullet -}) < -1.41$ V vs. Ag/AgNO$_3$ [6]. In view of the wide conjugation of BL and the strong electronic interaction across the bridging ligand, the reduction ability of the OER species ($E_{1/2}^{\mathrm{red}} = -1.1$ V vs. Ag/AgNO$_3$) should be insufficient for prompt reduction of CO_2 under these conditions.

According to the same strategy, they also recently developed photocatalytic CO_2 reduction systems using various multinuclear Ru complexes, which selectively produce HCOOH with high turnover numbers (~671) under visible light ($\lambda = 480$ nm) [19]. This kind of supramolecular metal complexes has been shown to be applicable to a Z-scheme CO_2 reduction system, in combination with a suitable semiconductor material, as will be discussed later.

2.3 Metal Complex Catalysts Based on Earth-Abundant Elements

Most of the metal complexes that have been developed to date for CO_2 reduction are comprised of Re- and Ru-based ones. In order to replace such precious metals from the sustainable chemistry point of view, an earth-abundant material that is sufficiently active, and alternative to precious metals, is highly desirable. Bourrez et al. reported that a manganese-based complex exhibited electrocatalytic activity for CO_2 reduction to CO, although the TON was moderate (TON = 13 for 4 h) [20]. Ishitani et al. used the same Mn complex as a catalyst, in combination with a ruthenium(II) tris-diimine complex as a redox sensitizer, to achieve CO_2 reduction into HCOOH in the presence of BNAH as an electron donor [21]. The QY of HCOOH formation by this Mn complex was 5.9 %, which is comparable to that achieved by a similar Re complex (6.9 %).

2.4 Enhanced Photocatalytic Activity of Rhenium(I) Complex by Light-Harvesting Periodic Mesoporous Organosilica

As briefly mentioned above, sunlight is a very “dilute” energy source (ca. 10 photons nm^{-2} s^{-1}) especially for small molecules such as metal complexes. Therefore, light-harvesting would be highly desirable for efficient photocatalysis by a homogeneous metal complex. In nature, a wheel-like array of chlorophylls in LH1 and LH2 of purple photosynthetic bacteria efficiently absorbs sunlight, funneling the captured energy to a reaction center by resonance energy transfer (RET) with a QY of almost unity [22]. For the construction of an artificial photosynthetic system, the three-dimensional organization of molecular parts, that is, light absorbers and multi-electron catalysts, at appropriate positions is of particular importance, because the RET efficiency is strongly dependent on the distance between the energy donor and acceptor molecules and their orientation [23].

Inagaki et al. employed a mesoporous biphenyl-silica (Bp-PMO) anchoring *fac*-$[Re^I(bpy)(CO)_3(PPh_3)]^+(OTf)^-$ (OTf = CF_3SO_3) in the mesochannels for CO_2 reduction [24]. The structure of this hybrid material is depicted in Fig. 2. The incident photons ($\lambda = 280$ nm) were effectively absorbed by the biphenyl groups in Bp-PMO, and the excited energy was funneled into the Re complex by RET. As the result, photocatalytic CO evolution from CO_2 was enhanced by a factor of 4.4, compared with direct excitation of the Re complex. In addition, Bp-PMO helped to protect the Re complex against photo-decomposition. These results demonstrate the potential of PMOs as a light-harvesting antenna for designing various photoreaction systems, mimicking the natural photosynthesis.

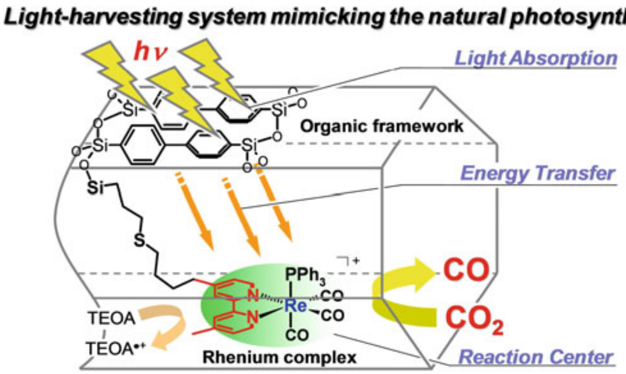

Fig. 2 Schematic representation of light-harvesting by PMO and enhancing of photocatalysis of Re complex. (Reprinted with permission from Ref. [24]. Copyright 2010, American Chemical Society)

3 Semiconductors

As described above, certain metal complexes catalyze CO_2 reduction to CO or HCOOH photocatalytically or electrochemically with high selectivity and QYs in a homogeneous system. From the viewpoint of large-scale application and efficient solar energy utilization, however, semiconductor-based heterogeneous photocatalysts would be more advantageous over molecular-based homogeneous catalysts, considering their superior oxidation ability to utilize a mild reductant (ideally, water) and potential recyclability [25]. In this section, several kinds of heterogeneous photocatalysts based on inorganic semiconductors for CO_2 reduction are described.

3.1 CO_2 Reduction on Wide Gap Semiconductors in the Presence of CH_4 or H_2

Tanaka et al. have developed several wide-gap semiconductors (some of them may be mentioned as insulators) such as ZrO_2 and MgO for CO_2 reduction into CO in the presence of CH_4 or H_2 gas as a reductant [26–28]. Their results indicated that CO_2 adsorbed on ZrO_2 and MgO, which are solid base oxides, is reduced to formate species by gas phase H_2. Importantly, the stable linear form of CO_2 transforms into a reactive species upon adsorption, which are more susceptible to reduction than the linear form.

Their group also reported that β-Ga_2O_3 having a band gap of ca. 4.5 eV showed higher activity for photocatalytic CO_2 reduction into CO in the presence of H_2 than other solid bases such as MgO [29]. This reaction is subject to a Langmuir-Hinshelwood type mechanism, where the monodentate bicarbonate species was

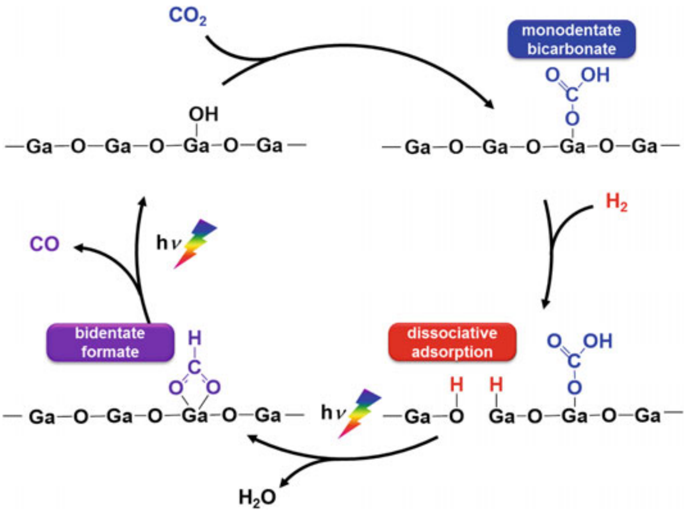

Scheme 4 Mechanism of photocatalytic reduction of CO_2 over β-Ga_2O_3 in the presence of H_2. (Reprinted with permission from Ref. [29]. Copyright 2010, American Chemical Society)

reduced by the dissociatively adsorbed hydrogen, thereby generating bidentate formate on β-Ga_2O_3 that was finally decomposed into CO under photo-irradiation (Scheme 4). Despite the inferior affinity of β-Ga_2O_3 with CO_2, the dissociatively adsorbed H_2 on β-Ga_2O_3 was responsible for the higher photocatalytic activity.

3.2 *Semiconductor Photocatalysts Workable in Water*

As described above, some of wide-gap semiconductor oxides (or insulators) have been shown to exhibit activity for CO_2 reduction into CO in the presence of CH_4 or H_2 as an electron donor. However, a semiconductor photocatalyst that is capable of reducing CO_2 using water as an electron source and of producing stoichiometric amount of O_2 had not been reported until recently.

In 2011, Kudo et al. reported that $ALa_4Ti_4O_{15}$ (A = Ca, Sr, and Ba) layered perovskites having 3.79–3.85 eV band gaps showed photocatalytic activity for CO_2 reduction to form CO and water oxidation into O_2 [30]. $ALa_4Ti_4O_{15}$ (A = Ca, Sr, and Ba) has been originally developed as a photocatalyst for overall water splitting into H_2 and O_2 under UV irradiation [31]. Table 1 summarizes the photocatalytic activities of $ALa_4Ti_4O_{15}$ (A = Ca, Sr, and Ba) for CO_2 reduction in water. While the CO_2 reduction activity was negligible in the absence of a cocatalyst, the activity could be enhanced by modification with Ag cocatalysts. Among three semiconductors tested, the Ba derivative was found to exhibit the highest performance. Under Ar bubbling condition, water splitting reaction proceeds on Ag/$BaLa_4Ti_4O_{15}$,

Table 1 Photocatalytic activities for CO_2 reduction over $ALa_4Ti_4O_{15}$ (A = Ca, Sr, and Ba) modified with Ag cocatalyst under UV irradiation ($\lambda > 200$ nm)[a]

Entry	Photocatalyst	Cocatalyst (wt%)	Loading method	Activity/μmol h^{-1}			
				H_2	O_2	CO	HCOOH
1	$CaLa_4Ti_4O_{15}$	0	–	1.3	0.6	0.07	0
2	$CaLa_4Ti_4O_{15}$	Ag (1.0)	Liquid-phase reduction	3.2	6.6	9.3	0.4
3	$SrLa_4Ti_4O_{15}$	0	–	0.8	0.5	0.06	0
4	$SrLa_4Ti_4O_{15}$	Ag (1.0)	Liquid-phase reduction	4.8	5.8	7.1	0.8
5	$BaLa_4Ti_4O_{15}$	0	–	5.3	2.4	0	0
6	$BaLa_4Ti_4O_{15}$	Ag (1.0)	Liquid-phase reduction	5.6	12	19	0.4
7	$BaLa_4Ti_4O_{15}$	Ag (1.0)	Impregnation[b]	5.6	8.7	8.9	0.3
8	$BaLa_4Ti_4O_{15}$	Ag (1.0)	Photodeposition	10	7.0	4.3	0.3
9[c]	$BaLa_4Ti_4O_{15}$	Ag (1.0)	Liquid-phase reduction	20	11	0	0

[a] Catalyst 0.3 g, water 360 mL, CO_2 flow system (15 mL min^{-1}), a 400 W high-pressure mercury lamp, an inner irradiation quartz cell

[b] Calcination at 723 K for 1 h in air, followed by reduction with H_2 at 473 K for 2 h

[c] Ar flow

but continuous CO_2 bubbling of the reactant solution allowed one to proceed CO_2 reduction into CO and HCOOH as the major and minor product, respectively. Although H_2 evolution via overall water splitting could not be suppressed completely, modification of $BaLa_4Ti_4O_{15}$ with ~10 nm Ag nanoparticles, which was achieved by employing the liquid-phase reduction method, improved the selectivity for CO_2 reduction while suppressing the undesirable H_2 evolution.

Even under CO_2 bubbling, cocatalysts of NiO_x, Ru, Cu, and Au did not achieve any appreciable CO_2 conversion, but promoted overall water splitting. Ag is known to be an efficient electrocatalyst for CO_2 reduction, but has relatively large overpotential for H_2 evolution [32]. This is a preferable feature for use as a cocatalyst for CO_2 reduction on a semiconductor photocatalyst, and appears to contribute to the superior performance of Ag-loaded material for CO_2 fixation. Kudo et al. also pointed out that continuous bubbling of the reactant suspension with CO_2 was important to get more CO, suggesting the occurrence of some backward reactions. It should be noted that in the optimal condition, the ratio of reduction/oxidation products $\{(CO + HCOOH + H_2)/O_2\}$ was almost equal to 2/1, consistent with the reaction stoichiometry. The stoichiometric evolution of O_2 clearly indicated that water was consumed as a reducing reagent (an electron donor) for the CO_2 reduction. Thus, an uphill reaction of CO_2 reduction accompanied with water oxidation was achieved using the $Ag/BaLa_4Ti_4O_{15}$ photocatalyst.

Teramura et al. have developed layered double hydroxides (LDHs; $[M^{2+}_{1-x}M^{3+}_{x}(OH)_2]^{x+}(A^{n-})_{x/n}\,mH_2O$) as new heterogeneous photocatalysts for CO_2 reduction

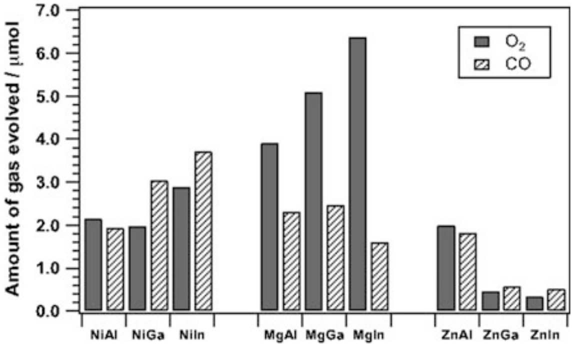

Fig. 3 Yields of O_2 and CO for the photocatalytic conversion of CO_2 in water, over various LDHs ($M^{2+}/M^{3+} = 3$) after 10 h of photo-irradiation ($\lambda > 200$ nm). (Reprinted with permission from Ref. [33]. Copyright 2011, Wiley–VCH Verlag GmbH and Co. KGaA)

workable in water under UV irradiation ($\lambda > 200$ nm) [33]. LDHs are natural or synthetic clays that consist of brucite ($Mg(OH)_2$)-like positively charged two-dimensional sheets interleaved with anionic species (A^{n-}) such as CO_3^{2-} for charge compensation, in which some divalent cations such as Mg^{2+} are substituted by trivalent cations. Although the reaction products did not meet the stoichiometry (in most cases, excess O_2 evolution was observed) and the reason still remains unclear, several kinds of LDHs showed activity for CO and O_2 evolution in water, as shown in Fig. 3. As exemplified by Mg-In LDH, interestingly, neither Mg- nor In-hydroxide gave CO or O_2 from water in the presence of CO_2, but the combination of the two metals to make a Mg-In LDH resulted in clearly observable CO and O_2 evolution. It indicates the importance of the formation of LDH structure for driving CO_2 reduction in water. They also conducted isotope tracer experiments with $^{13}CO_2$, which indicated that the main source of CO generated was CO_2 molecules in gas phase, but some residual CO_3^{2-} ions in the interlayer became the source of CO.

4 Metal-Complex/Semiconductor Hybrid Photocatalysts

4.1 *The Proof-of-Concept*

As introduced above, certain metal complexes based on rhenium or ruthenium catalyze CO_2 reduction to CO or HCOOH (photo)catalytically with high selectivity and QYs. However, the oxidation ability of these metal complexes is in general too low to oxidize water. By contrast, while the selectivity for CO_2 reduction is not very high, the stability of semiconductors for oxidation reactions is attractive.

On the basis of these backgrounds, one can simply draw a composite material, as shown in Scheme 5, consisting of a light-absorbing semiconductor and a catalytic

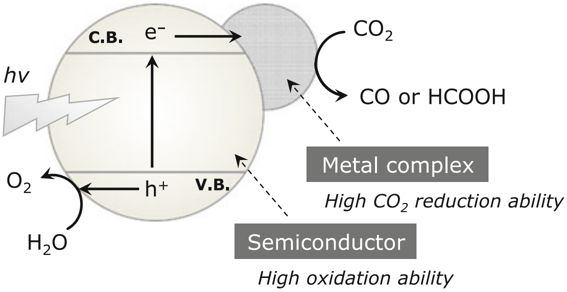

Scheme 5 Photocatalytic CO$_2$ reduction and water oxidation on a metal complex/semiconductor hybrid. V.B. and C.B. indicate the valence and conduction band of a semiconductor, respectively

metal complex, which shows high performance both for water oxidation and CO$_2$ reduction. In 2010, Morikawa et al. reported a proof-of-concept of this kind of a metal-complex/semiconductor hybrid photocatalyst to reduce CO$_2$ into formic acid [34]. They used a p-type semiconductor, N-doped Ta$_2$O$_5$ (energy gap = ca. 2.6 eV), and ruthenium(II) complexes $[Ru(bpy)_2(CO)_2]^{2+}$, $[Ru(dcbpy)(bpy)(CO)_2]^{2+}$ or $[Ru(dcbpy)_2(CO)_2]^{2+}$ (dcbpy: 4,4′-dicarboxy-2,2′-bipyridine; bpy: 2,2′-bipyridine). $[Ru(dcbpy)_2(CO)_2]^{2+}$ is an electrocatalyst for CO$_2$ reduction into HCOOH [35]. Under irradiation of the composite with visible light in a mixed solution of acetonitrile (MeCN) and TEOA, electrons and holes are generated in the conduction and valence band of N-Ta$_2$O$_5$, respectively. Here, the adsorbed metal complexes do not essentially harvest the incident photons. The conduction band electrons move to the adsorbed Ru complex, thereby reducing CO$_2$ into HCOOH. On the other hand, holes left behind the valence band are consumed by oxidation of TEOA. The selectivity of HCOOH production was more than 75 % before the turnover number underwent saturation. Unfortunately, however, N-Ta$_2$O$_5$ is unable to oxidize water into molecular O$_2$ because the valence band potential is more negative than the water oxidation potential. Therefore, this system is not applicable to an artificial photosynthetic assembly using water as an electron source.

4.2 *Metal-Complex/Polymeric Semiconductor Hybrid*

As an alternative semiconductor material that has stronger oxidation ability, Maeda et al. focused on carbon nitride polymers [36, 37]. Carbon nitride is an earth-abundant polymer semiconductor photocatalyst, which has recently been developed for water splitting with visible light by the same group [38, 39]. It has several proposed allotropes with diverse properties, but the graphitic phase is regarded as the most stable under ambient conditions. Graphitic carbon nitride is yellow powder with high chemical stability both in acid and base, exhibiting a steep absorption edge at around 450 nm and a tail extending to 600 nm. Importantly, the material shows photocatalytic activity for water oxidation, in contrast to nitrogen doped Ta_2O_5. However, there had been no reliable report on photocatalytic CO_2 reduction using C_3N_4 as a photocatalyst until very recently.

Mesoporous graphitic carbon nitride (mpg-C_3N_4) polymers with a ruthenium complex, *cis, trans*-[Ru{4,4′-$(CH_2PO_3H_2)_2$-2,2′-bipyridine}$(CO)_2Cl_2$] (abbreviated **Ru** for simplicity), that works a catalyst for CO_2 reduction were combined together to create a new CO_2 reduction photo-assembly [36]. Table 2 summarizes CO_2 reduction activities, which were tested in a MeCN–TEOA mixture (4:1 v/v) under >400 nm irradiation. Mpg-C_3N_4 alone did not show any activity for CO_2 reduction. However, combining mpg-C_3N_4 with **Ru** resulted in the production of HCOOH and CO as CO_2 reduction products, with H_2 as a byproduct. Under optimal condition, turnover number with respect to the adsorbed **Ru** exceeded 200 after 20 h of visible light irradiation, with selectivity of formic acid production of higher than 80 %. These numbers are higher than those recorded by the previous report using nitrogen doped Ta_2O_5. Control experiments showed that using an insulator, alumina, instead of carbon nitride, did not give any products. Nothing happened without catalyst sample as well. When the reaction was conducted under argon atmosphere, no carbon-containing product was obtained, evolving H_2 alternatively. Without TEOA, the amounts of produced HCOOH and CO became very low.

Figure 4 shows an action spectrum of formic acid production on **Ru**/mpg-C_3N_4. The apparent quantum yield (AQY) decreased with increasing the wavelength of incident light, and reached zero at 550 nm. This change in AQY corresponds to the light-absorption profile of carbon nitride, which is shown by red curve. It clearly means that the formic acid production originates from light absorption by carbon nitride. Because **Ru**/mpg-C_3N_4 photocatalyst consists of large amount of carbon, isotope tracer experiments were conducted using $^{13}CO_2$ as the reactant. Interestingly, the main product of HCOOH was found to originate solemnly from

Table 2 Photocatalytic activities for CO_2 reduction over **Ru**/mpg-C_3N_4 in a CO_2-saturated $MeCN^-$–TEOA mixed solution under visible light (λ > 400 nm)[a]

Entry	Photocatalyst	Solution	Amount of products (5 h)/nmol		
			H_2	CO	HCOOH
1	mpg-C_3N_4	MeCN–TEOA	354	0	0
2	**Ru**/mpg-C_3N_4	MeCN–TEOA	1267	580	5455
3	**Ru**/Al_2O_3	MeCN–TEOA	7	0	0
4	None	MeCN–TEOA	0	0	0
5[b]	**Ru**/mpg-C_3N_4	MeCN–TEOA	3772	0	0
6	**Ru**/mpg-C_3N_4	MeCN	0	160	110

[a] Catalyst 8.0 mg (**Ru** 7.8 μmol g^{-1} adsorbed), MeCN–TEOA mixed solution (4:1 v/v) 4 mL, a 450 W high-pressure mercury lamp with a $NaNO_2$ solution filter, a Pyrex test tube cell (11 mL capacity)

[b] Ar atomsphere. (Reproduced with permission from Ref. [36]. Copyright 2013, The Royal Society of Chemistry)

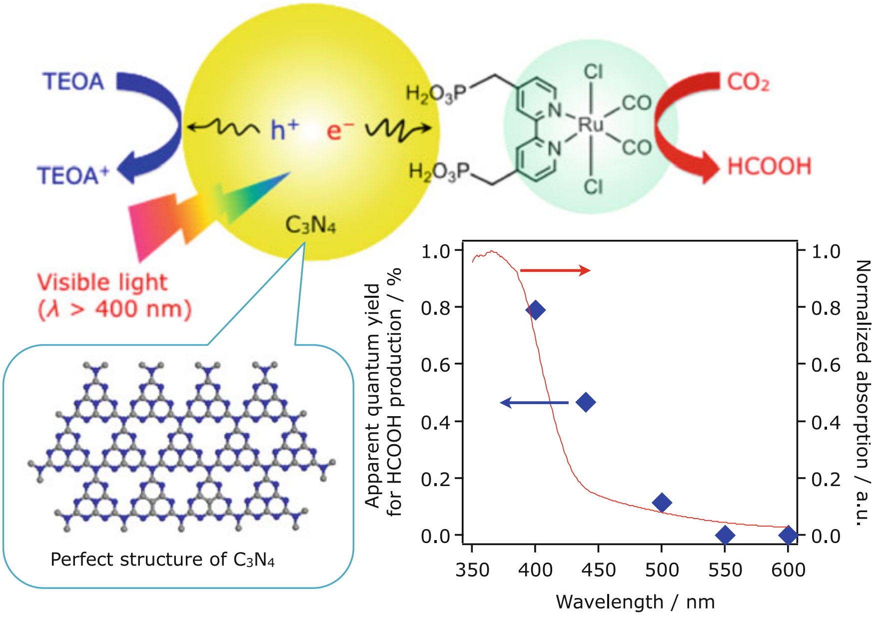

Fig. 4 Schematic illustration of photocatalytic CO_2 reduction into HCOOH on **Ru**/mpg-C_3N_4 under visible light, along with the action spectrum. (Reproduced with permission from Ref. [36]. Copyright 2013, The Royal Society of Chemistry)

CO_2, not the decomposition of C_3N_4 component. Based on these results, it was concluded that **Ru** and carbon nitride work as CO_2 reduction catalyst and light-absorber, respectively. Also, TEOA is an electron donor to scavenge holes in the valence band of carbon nitride, and a proton source.

In contrast to inorganic semiconductors, it is possible to control both bulk and surface properties of C_3N_4 based on an organic chemistry protocol [40], thereby modulating the band-gap structure and introducing a desired organic moiety that anchors a metal-complex catalyst. Besides, C_3N_4 is structurally flexible, exhibiting various shapes with the aid of a hard template such as silica during the synthesis [41]. Maeda et al. have also reported that the activity of **Ru**/C_3N_4 for the CO_2 reduction reaction is sensitive to specific surface area and crystallinity of carbon nitride, but is largely insensitive to the pore size and the volume [37].

4.3 Artificial Z-Scheme

Very recently, Ishitani et al. developed a new type of photocatalytic CO_2 fixation system using Ag-loaded TaON semiconductor and a Ru(II) binuclear complex, which works according to Z-scheme principle somewhat similar to natural

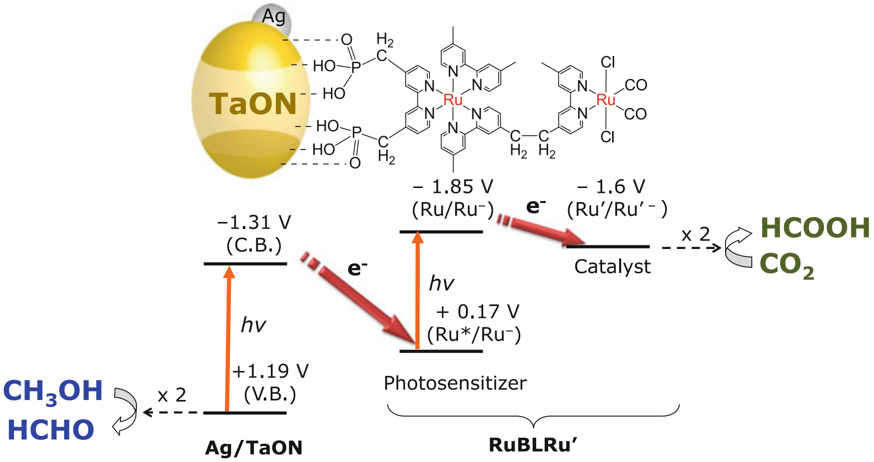

Scheme 6 Artificial Z-scheme for photocatalytic CO_2 reduction using Ag-loaded TaON semiconductor and a Ru(II) binuclear complex (RuBLRu′). (Reproduced with permission from Ref. [42]. Copyright 2013, American Chemical Society)

photosynthesis in green plants [42]. As illustrated in Scheme 6, two components of TaON and light-harvesting Ru unit both undergo photoexcitation upon visible light in the initial step. The photogenerated hole in the TaON valence band oxidizes methanol, and the conduction band electrons move to the excited or oxidized photosensitizer unit, but cannot be transferred to the ground state. An OER species generated as a result of the interfacial electron transfer is consumed by intramolecular electron transfer, which is thermodynamically down-hill, finally reducing CO_2 into HCOOH on the catalytic Ru unit. Because formic acid production from CO_2 involves a two-electron reduction, the stepwise two-photon absorption and subsequent electron transfer processes would occur twice during the reduction of CO_2 to give one HCOOH molecule. It should be noted that the whole reaction is energetically up-hill, involving a positive change in the Gibbs energy of 83.0 kJ mol^{-1}. Isotope tracer experiments indicated that this hybrid material photocatalytically produced formic acid as the major reduction product and formaldehyde as the oxidation product from CO_2 and methanol, respectively. Under visible light ($\lambda > 400$ nm), both Ag/TaON and the sensitizer unit in the supramolecular complex undergo photoexcitation. The conduction band electrons in Ag/TaON migrate to the excited state or oxidized sensitizer unit, producing a one-electron reduced species. Subsequent intermolecular electron transfer occurs from the one-electron- reduced species in the photosensitizer unit to the catalyst unit, as it is a thermodynamically downhill process. Finally, holes left in the valence band of Ag/TaON oxidize methanol to give formaldehyde, whereas electrons transferred to the catalyst unit reduce CO_2 into formic acid. Since the CO_2 reduction to give formic acid is a two-electron process, the stepwise two-photon absorption and the subsequent electron transfer events are likely to occur twice during the reaction to give one HCOOH molecule.

Currently, the main problem of this Z-scheme system includes competitive H_2 evolution that lowers the selectivity of CO_2 reduction, significant electron–hole recombination in the TaON component [43], and possible back electron transfer from the excited-state photosensitizing unit to Ag/TaON, which is thermodynamically a down-hill process. To address these problems, refinement of preparation condition of TaON as well as proper design of the metal complex component to maximize the forward electron transfer rate is required. In addition, role(s) of Ag deposits on TaON need to be clarified, as the efficiency of this system becomes very low in the absence of the Ag modification.

5 Summary and Future Outlook

In this chapter, photocatalytic CO_2 reduction both in homogeneous and heterogeneous systems are reviewed. Certain metal complexes consisting rhenium, ruthenium, or manganese are shown to work as efficient (photo)catalysts for CO_2 reduction into CO or HCOOH with high quantum yields and selectivity. Unfortunately, however, no metal complex that is capable of oxidizing water to drive CO_2 reduction has been reported so far. On the other hand, semiconductor photocatalysts having high photooxidation ability could be applicable to a CO_2 reduction system that should utilize water as an electron source. For example, $ALa_4Ti_4O_{15}$ (A = Ca, Sr, and Ba) modified with Ag nanoparticles exhibit activity for CO_2 reduction and water oxidation under band-gap irradiation. A suitable combination between a metal complex and a semiconductor led to the development of new visible-light CO_2 reduction systems. Importantly, some of them could work non-sacrificially, converting visible-light energy into chemical energy.

References

1. Morris AJ, Meyer GJ, Fujita E (2009) Molecular approaches to the photocatalytic reduction of carbon dioxide for solar fuels. Acc Chem Res 42:1983–1994
2. Takeda H, Ishitani O (2010) Development of efficient photocatalytic systems for CO_2 reduction using mononuclear and multinuclear metal complexes based on mechanistic studies. Coord Chem Rev 254:346–354
3. Hawecker J, Lehn J-M, Ziessel R (1983) Efficient photochemical reduction of CO_2 to CO by visible light irradiation of systems containing $Re(bipy)(CO)_3X$ or $Ru(bipy)_3^{2+}$–Co^{2+} combinations as homogeneous catalysts. J Chem Soc Chem Commun 536–538
4. Yui T, Kan A, Saitoh C, Koike K, Ibusuki T, Ishitani O (2011) Photochemical reduction of CO_2 using TiO_2: effects of organic adsorbates on TiO_2 and deposition of Pd onto TiO_2. ACS Appl Mater Interfaces 3:2594–2600
5. Hori H, Koike K, Ishizuka M, Takeuchi K, Ibusuki T, Ishitani O (1997) Preparation and characterization of $[Re(bpy)(CO)_3L][SbF_6]$ (L = phosphine, phosphite). J Organomet Chem 530:169–176

6. Koike K, Hori H, Ishizuka M, Westwell JR, Takeuchi K, Ibusuki T, Enjouji K, Konno H, Sakamoto K, Ishitani O (1997) Key process of the photocatalytic reduction of CO_2 using [Re (4,4-X_2-bipyridine)$(CO)_3PR_3]^+$ (X = CH_3, H, CF_3; PR_3 = Phosphorus Ligands): dark reaction of the one-electron-reduced complexes with CO_2. Organometallics 16:5724–5729
7. Hori H, Johnson FPA, Koike K, Ishitani O, Ibusuki T (1996) Efficient photocatalytic CO_2 reduction using $[Re(bpy)(CO)_3\{P(OEt)_3\}]^+$. J Photochem Photobiol A Chem 96:171–174
8. Takeda H, Koike K, Inoue H, Ishitani O (2008) Development of an efficient photocatalytic system for CO_2 reduction using rhenium(I) complexes based on mechanistic studies. J Am Chem Soc 130:2023–2031
9. Kutal C, Weber MA, Ferraudi G, Geiger D (1985) A mechanistic investigation of the photoinduced reduction of carbon dioxide mediated by tricarbonylbromo(2,2’-bipyridine) rhenium(I). Organometallics 4:2161–2166
10. Kalyanasundaram K (1986) Luminescence and redox reactions of the metal-to-ligand charge-transfer excited state of tricarbonylchloro-(polypyridyl)rhenium(I) complexes. J Chem Soc Faraday Trans 2(82):2401–2415
11. Kutal C, Corbin AJ, Ferraudi G (1987) Further studies of the photoinduced reduction of carbon dioxide mediated by tricarbonylbromo(2,2′-bipyridine)rhenium(I). Organometallics 6:553–557
12. Smieja JM, Benson EE, Kumar B, Grice KA, Seu CS, Miller AJM, Mayer JM, Kubiak CP (2012) Kinetic and structural studies, origins of selectivity, and interfacial charge transfer in the artificial photosynthesis of CO. Proc Natl Acad Sci 109:15646–15650
13. Smieja JM, Kubiak CP (2010) Re(bipy-tBu)$(CO)_3Cl^-$improved catalytic activity for reduction of carbon dioxide: IR-spectroelectrochemical and mechanistic studies. Inorg Chem 49:9283–9289
14. Hayashi Y, Kita S, Brunschwig BS, Fujita E (2003) Involvement of a binuclear species with the Re−C(O)O−Re moiety in CO_2 reduction catalyzed by tricarbonyl rhenium(I) complexes with diimine ligands: strikingly slow formation of the Re−Re and Re−C(O)O−Re species from Re(dmb)(CO)3S (dmb = 4,4′-Dimethyl-2,2′-bipyridine, S = Solvent). J Am Chem Soc 125:11976–11987
15. Agarwal J, Fujita E, Schaefer HF III, Muckerman JT (2012) Mechanisms for CO Production from CO_2 using reduced rhenium tricarbonyl catalysts. J Am Chem Soc 134:5180–5186
16. Lehn J-M, Ziessel R (1982) Photochemical generation of carbon monoxide and hydrogen by reduction of carbon dioxide and water under visible light irradiation. Proc Natl Acad Sci 79:701–704
17. Morimoto T, Nakajima T, Sawa S, Nakanishi R, Imori D, Ishitani O (2013) CO_2 capture by a rhenium(I) complex with the aid of triethanolamine. J Am Chem Soc 135:16825–16828
18. Gholamkhass B, Mametsuka H, Koike K, Tanabe T, Furue M, Ishitani O (2005) Architecture of supramolecular metal complexes for photocatalytic CO_2 reduction: Rutheniu−rhenium Bi-and tetranuclear complexes. Inorg Chem 44:2326–2336
19. Tamaki Y, Morimoto T, Koike K, Ishitani O (2012) Photocatalytic CO_2 reduction with high turnover frequency and selectivity of formic acid formation using Ru(II) multinuclear complexes. Proc Natl Acad Sci 109:15673–15678
20. Bourrez M, Molton F, Chardon-Noblat S, Deronzier A (2012) [Mn(bipyridyl)$(CO)_3$Br]: an abundant metal carbonyl complex as efficient electrocatalyst for CO_2 reduction. Angew Chem Int Ed 50:9903–9906
21. Takeda H, Koizumi H, Okamoto K, Ishitani O (2014) Photocatalytic CO_2 reduction using a Mn complex as a catalyst. Chem Commun 50:1491–1493
22. Pullerits T, Sundström V (1996) Photosynthetic light-harvesting pigment-protein complexes: toward understanding how and why. Acc Chem Res 29:381–389
23. Alstrum-Acevedo JH, Brennaman MK, Meyer TJ (2005) Chemical approaches to artificial photosynthesis. 2. Inorg Chem 44:6802–6827
24. Takeda H, Ohashi M, Tani T, Ishitani O, Inagaki S (2010) Enhanced photocatalysis of rhenium(I) complex by light-harvesting periodic mesoporous organosilica. Inorg Chem 49:4554–4559

25. Maeda K (2011) Photocatalytic water splitting using semiconductor particles: History and recent developments. J Photochem Photobiol C: Reviews 12:237–268
26. Kohno Y, Tanaka T, Funabiki T, Yoshida S (1997) Photoreduction of carbon dioxide with methane over ZrO_2. Chem Lett 993–994
27. Kohno Y, Ishikawa H, Tanaka T, Funabiki T, Yoshida S (2001) Photoreduction of carbon dioxide by hydrogen over magnesium oxide. Phys Chem Chem Phys 3:1108–1113
28. Teramura K, Tanaka T, Ishikawa H, Kohno Y, Funabiki T (2004) Photocatalytic reduction of CO_2 to CO in the presence of H_2 or CH_4 as a reductant over MgO. J Phys Chem B 108:346–354
29. Tsuneoka H, Teramura K, Shishido T, Tanaka T (2010) Adsorbed species of CO_2 and H_2 on Ga_2O_3 for the photocatalytic reduction of CO_2. J Phys Chem C 114:8892–8898
30. Iizuka K, Wato T, Miseki Y, Saito K, Kudo A (2011) Photocatalytic reduction of carbon dioxide over Ag cocatalyst-loaded $ALa_4Ti_4O_{15}$ (A = Ca, Sr, and Ba) using water as a reducing reagent. J Am Chem Soc 133:20863–20868
31. Miseki Y, Kato H, Kudo A (2009) Water splitting into H_2 and O_2 over niobate and titanate photocatalysts with (111) plane-type layered perovskite structure. Energy Environ Sci 2:306–314
32. Hori Y, Wakabe H, Tsukamoto T, Koga O (1994) Electrocatalytic process of CO selectivity in electrochemical reduction of CO_2 at metal electrodes in aqueous media. Electrochim Acta 39:1833–1839
33. Teramura K, Iguchi S, Mizuno Y, Shishido T, Tanaka T (2012) Photocatalytic conversion of CO_2 in water over layered double hydroxides. Angew Chem Int Ed 51:8008–8011
34. Sato S, Morikawa T, Saeki S, Kajino T, Motohiro T (2010) Visible-light-induced selective CO_2 reduction utilizing a ruthenium complex electrocatalyst linked to a p-type nitrogen-doped Ta_2O_5 semiconductor. Angew Chem Int Ed 49:5101–5105
35. Ishida H, Tanaka K, Tanaka T (1987) Electrochemical CO_2 reduction catalyzed by ruthenium complexes $[Ru(bpy)_2(CO)_2]^{2+}$ and $[Ru(bpy)_2(CO)Cl]^+$. Effect of pH on the formation of CO and $HCOO^-$. Organometallics 6:181–186
36. Maeda K, Sekizawa K, Ishitani O (2013) A polymeric-semiconductor–metal-complex hybrid photocatalyst for visible-light CO_2 reduction. Chem Commun 49:10127–10129
37. Maeda K, Kuriki R, Zhang M, Wang X, Ishitani O (2014) The effect of the pore-wall structure of carbon nitride on photocatalytic CO_2 reduction under visible light. J Mater Chem A 2:15146–15151
38. Wang X, Maeda K, Thomas A, Takanabe K, Xin G, Carlsson JM, Domen K, Antonietti M (2009) A metal-free polymeric photocatalyst for hydrogen production from water under visible light. Nat Mater 8:76–80
39. Maeda K, Wang X, Nishihara Y, Lu D, Antonietti M, Domen K (2009) Photocatalytic activities of graphitic carbon nitride powder for water reduction and oxidation under visible light. J Phys Chem C 113:4940–4947
40. Zhang J, Chen X, Takanabe K, Maeda K, Domen K, Fu X, Antonietti M, Wang X (2010) Synthesis of a carbon nitride structure for visible-light catalysis by copolymerization. Angew Chem Int Ed 49:441–444
41. Goettmann F, Fischer A, Antonietti M, Thomas A (2006) Chemical synthesis of mesoporous carbon nitrides using hard templates and their use as a metal-free catalyst for friedel-crafts reaction of benzene. Angew Chem Int Ed 45:4467–4471
42. Sekizawa K, Maeda K, Koike K, Domen K, Ishitani O (2013) Artificial Z-scheme constructed with a supramolecular metal complex and semiconductor for the photocatalytic reduction of CO_2. J Am Chem Soc 135:4596–4599
43. Maeda K, Higashi M, Lu D, Abe R, Domen K (2010) Efficient nonsacrificial water splitting through two-step photoexcitation by visible light using a modified oxynitride as a hydrogen evolution photocatalyst. J Am Chem Soc 132:5858–5868